ORIGINAL ARTICLE

CrossMark

Characterization and Cytotoxicity Evaluation of a Marine Sponge Biosilica

P. R. Gabbai-Armelin[1] · H. W. Kido[1] · M. A. Cruz[1] · J. P. S. Prado[1] · I. R. Avanzi[1] · M. R. Custódio[2] · A. C. M. Renno[1] · R. N. Granito[1]

Abstract
Bone fractures characterize an important event in the medical healthcare, being related to traumas, aging, and diseases. In critical conditions, such as extensive bone loss and osteoporosis, the tissue restoration may be compromised and culminate in a non-union consolidation. In this context, the osteogenic properties of biomaterials with a natural origin have gained prominence. Particularly, marine sponges are promising organisms that can be exploited as biomaterials for bone grafts. Thus, the objectives of this study were to study the physicochemical and morphological properties of biosilica (BS) from sponges by using scanning electron microscopy, Fourier-transform infrared, X-ray diffraction (SEM, FTIR and XRD respectively), mineralization, and pH. In addition, tests on an osteoblast precursor cell line (MC3T3-E1) were performed to investigate its cytotoxicity and proliferation in presence of BS. Bioglass (BG) was used as gold standard material for comparison purposes. Sponge BS was obtained, and this fact was proven by SEM, FTIR, and XRD analysis. Calcium assay showed a progressive release of this ion from day 7 and a more balanced pH for BS was maintained compared to BG. Cytotoxicity assay indicated that BS had a positive influence on MC3T3-E1 cells viability and qRT-PCR showed that this material stimulated Runx2 and BMP4 gene expressions. Taken together, the results indicate a potential use of sponge biosilica for tissue engineering applications.

Introduction

Bone fractures represent a critically important event in the medical practice and it is related mainly to traumas, accidents, aging, sports injuries, and diseases (Hak et al. 2014). Previous data demonstrated an annual incidence of 21 fractures per 1000 people in the USA, contributing to an increase in morbidity, disability, and healthcare costs (Pressley et al. 2011).

In general, after an injury, bone tissue has the ability of healing by itself (Matassi et al. 2011; Tsiridis et al. 2007).

P. R. Gabbai-Armelin and H. W. Kido equally contributed to this paper.

✉ P. R. Gabbai-Armelin
paulogabbai@gmail.com

1 Laboratory of Biomaterials and Tissue Engineering, Department of Biosciences, Federal University of São Paulo (UNIFESP), Silva Jardim, 136, Santos, SP 11015-020, Brazil

2 Laboratory of Marine Invertebrates Cell Biology, Institute of Biosciences, University of São Paulo (USP), Rua do Matão, 101, São Paulo, SP 05508-900, Brazil

However, in critical conditions, such as extensive loss of bone, critical defects, and fractures related to diseases like osteoporosis, the consolidation process may be impaired and culminate in a compromised healing or even in a non-union consolidation (Nukavarapu and Dorcemus 2013).

Based on these statements, it is clear that the development of innovative strategies capable of stimulating bone metabolism would decrease the chances of bone fracture complications from abnormal repair process (Henkel et al. 2013).

In this context, different biomaterials have been emerging as promising therapeutic interventions able of stimulating bone tissue, mainly due to their osteogenic effects (Matassi et al. 2011). Natural or synthetic materials provide a specific environment and architecture, in terms of neovascularization and osteoinduction, for bone tissue repair (Matassi et al. 2013). Nowadays, the osteogenic effects of biomaterials with a natural origin have gained prominence. Many authors state that they are more biocompatible and provide a more appropriate surface for cell attachment and growth when compared to synthetic biomaterials (Lin et al. 2011; Muller et al. 2013a; Wang et al. 2014). In this context, the rich

marine biodiversity provides a plentiful resource of metabolites and molecules to be used as raw materials for new pharmaceutical and therapeutic products (Radjasa et al. 2011). In particular, marine sponges, with their unique composition and structure, are considered one of the most promising organisms that can be exploited as biomaterials for bone grafts (Granito et al. 2017; Lin et al. 2011). The inorganic skeleton of most marine sponges is composed by spicules, discrete structures made by biosilica (BS), a biocompatible, natural polymer formed by an enzymatic, and silicatein-mediated reaction (Muller et al. 2010; Wang et al. 2014). Some authors have obtained BS from sponges and demonstrated in vitro evidences of osteogenic activity, through the upregulation of genes related to bone cell proliferation and differentiation, together with its ability to stimulate mineralization (Muller et al. 2010; Wang et al. 2014).

Following this line, Zhu et al. (2018) studied the influence of BS porous microsphere consisting of poly(lactic-co-glycolic acid)/beta-tricalcium phosphate coated with silica and silicatein on the growth and osteogenic differentiation of human dental pulp cell (hDPCs). The novel biomicrospheres supported the attachment and expansion of hDPCs, upregulated the expression of collagen type I and dentin sialophosphoprotein, and promoted alkaline phosphatase secretion in the environment (Zhu et al. 2018). Moreover, Albert et al. (2017) and Granito et al. (2017) have reviewed the use of natural marine sponges and BS composites for biomedical applications due to their unique structural (interconnected porous architecture), chemical, and biological properties, focusing on relevant applications in bone tissue engineering, drug delivery systems, and biosensing (Albert et al. 2017; Granito et al. 2017). In another research, the authors explored a diatom biosilica and showed that the amorphous biomaterial is non-cytotoxic and supports cell proliferation and growth, offering a platform for biomedical therapeutics (Walsh et al. 2017). Also investigating biosilica, Leone et al. (2017) doped this mesoporous BS with Ca^{2+} and, via viability studies, showed an ameliorative effect on SaOS-2 cells spreading compared with cells grown on non-dope BS supports (Leone et al. 2017).

Despite all these positive evidences of BS toward the stimulation of bone tissue, many of the physicochemical and structural characteristics, cytocompatibility, and osteogenic activity are not well known yet. Thus, our aims were to investigate the physicochemical and morphological properties of BS by using scanning electron microscopy, Fourier-transform infrared, X-ray diffraction (SEM, FTIR, and XRD respectively), mineralization, and pH, and to study its cytotoxicity and the influence on cell proliferation, through in vitro tests. The well-known bioglass (BG) (Granito et al. 2017; Hench 2006) was used as gold standard material, as our aim was also to compare the biological performance sponge BS with the material with the highest known bioactive properties. We hypothesized that BS would also present good osteogenic properties to be used as a new substrate for bone tissue engineering applications.

Materials and Methods

Materials

Biosilica Preparation

BS was isolated from specimens of the marine sponge *Tedania ignis* and *Dragmacidon reticulatum* collected in São Sebastião, north coast of São Paulo state, Brazil. The sponges were cut into small pieces and washed with Milli-Q water. Firstly, the samples were treated with 5% (*v/v*) sodium hypochlorite to degrade all organic matter. Then, the material was washed 10 times with Milli-Q water to remove the sodium hypochlorite solution. After this, the material was transferred into a beaker containing a solution of nitric acid/sulfuric acid (1:4) to remove any remaining organic residue. Finally, several washes were performed using Milli-Q water to reach a final pH > 6.0 (Weaver et al. 2003). After all, BS samples were dried at room temperature and the range of particles was selected by sieves, resulting in a fine powder (particle size: 106–126 μm).

Bioglass

Amorphous BG, belonging to the system SiO_2-CaO-Na_2O-P_2O_5 (Hench 2006; Hench 2013), was produced and provided by Nuclear and Energy Research Institute (particle size: 106–126 μm; IPEN, São Paulo, Brazil).

Material Characterization

Scanning Electron Microscopy

The BS and BG samples were mounted on aluminum stubs using carbon tape and sputter-coated with gold/palladium (System BAL-TEC MED 020, BAL-TEC, Liechtenstein) and examined by SEM using a ZEISS LEO 440 microscope (20 kV, 2.82 A).

Fourier-Transform Infrared Spectroscopy

FTIR (Perkin-Elmer 1700 UK) was executed to depict the chemical bonds present in the BS and BG. Analyses were done in the range of 400–4000 cm^{-1} with a resolution of 2 cm^{-1}. The samples were scanned 100 times for each FTIR measurement and the spectrum acquired was the average of all these scans.

X-Ray Diffraction

XRD (Philips, Cu-Ka, 45 kV, 30 mA) patterns of the materials were collected, in the 2θ range of 5–65º, to analyze the crystalline structures in the sample.

Ca Assay in Simulated Body Fluid

The mineralization behavior of BS and BG samples was assessed in vitro by following the methods described by Kokubo and Takadama (2006). SBF was prepared under laminar flow to prevent contamination, having an ionic composition almost equal to human plasma. Ionic concentrations of the SBF were 142.0 mM Na^+, 5.0 mM K^+, 1.5 mM Mg^{2+}, 2.5 mM Ca^{2+}, 147.8 mM Cl^-, 4.2 mM HCO_3^{-2}, 1.0 mM HPO_4^-, and 0.5 mM SO_4^{-2}. Tris-HCl served as a buffer to keep a constant pH value of 7.4. The samples of BS (1.109 g; $n = 5$) and BG powders (1.109 g; $n = 5$) were placed in glass vials containing 15 mL of SBF at 37 °C on a shaker table (70 Hz) for up to 21 days, with refreshment on days 1, 3, 7, 14, and 21. In each period, the solution was collected for analysis of the calcium content in SBF by the orthocresolphtalein complexone (OCPC) assay (Mooren et al. 2010). Briefly, the solutions were incubated overnight in 500 μL of 0.5 N acetic acid on a shaker table. For analysis, 300 μL working reagent was added to 10 μL sample or standard in a 96-well plate. The plate was incubated for 10 min at room temperature. The absorbance of each well was measured on a microplate spectrophotometer at 570 nm (Bio-Tek Instruments, Winooski, VT, USA). The standards were prepared using a $CaCl_2$ stock solution. Data were obtained from quintuplicate samples and measured in duplo. The depletion of Ca was plotted cumulatively, measuring the difference between the Ca concentration in the sample-free SBF control solutions and the Ca concentration of SBF solution in the presence of BG and BS.

pH Measurements

After 1, 3, 7, 14, and 21 days of incubation in SBF, the pH of BG and BS was measured ($n = 5$) using a pH electrode (Orion Star A211, Thermo Scientific, Massachusetts, USA). The initial value for pH measurements was 7.4, corresponding to the pH of the SBF.

Cell Culture Studies

Cytotoxicity of BG and BS and their influence on cell proliferation was assessed by an indirect assay (Shin et al. 2003) using extracts of the materials. For this purpose, the materials were sterilized using ultraviolet irradiation (UV) for 24 h. Then, BG or BS (0.1, 0.05, and 0.01 g/mL; $n = 5$) was incubated in standard α-MEM culture medium (alpha minimal essential medium with 10% fetal bovine serum and 1% antibiotic; Vitrocell, Campinas, Brazil) supplemented with 1% β-glycerophosphate, 1% 2-phospho-L-ascorbic acid trisodium salt, and 0.1% dexamethasone for 24 h in a humidified incubator set at 37 °C and 5% CO_2 (ANSI 1999). After this period, these conditioned media were collected and filtered using a 0.22-μm filter (Kasvi, Curitiba, Brazil). Control without material was incubated under the same conditions described above.

MC3T3-E1 cells (BCRJ, RJ, Brazil) were cultured in standard culture medium using a humidified incubator set at 37 °C and 5% CO_2. Upon 80% confluency, cells were detached using trypsin and seeded at a density of 5×10^3 cells/cm^2 in 24-well plates containing 1 mL of supplemented standard medium per well. After 24 h, this was substituted for 1 mL of the conditioned media previously collected, and the cells were incubated for 1, 3, and 6 days. Afterwards, alamarBlue® assay (Thermo Fisher Scientific, São Paulo, Brazil) was performed on all samples, at each time point, in order to evaluate cell viability. For this analysis, 500 μL of 10% alamarBlue® solution was added into each well and incubated in dark for 3 h. After, 200 μL of solution (in duplicate) were aliquoted into wells of a 96-well plate for the measurements in the microplate spectrophotometer (Bio-Tek Instruments, Inc.) at 570 and 600 nm. From the values obtained, proliferation rates were calculated as the percentage reduction of alamarBlue®, according to manufacturer's instructions.

Subsequently, the alamarBlue® solution in contact with cells was washed away twice using PBS and the same well plate, at each experimental period, was used for DNA quantification by PicoGreen assay (QuantiFluor® dsDNA quantification kit; Promega, São Paulo, Brazil). After two freeze-thaw cycles (-80 °C and 25 °C), 100 μL of freshly made working solution was added into each well which contained 100 μL of sample or DNA standard, and the plate was stored in the dark for 5 min. Finally, the fluorescent signal (485/20 excitation and 528/20 emission) was read using the microplate spectrophotometer (Bio-Tek Instruments, Inc.).

Quantitative RT-PCR

In order to evaluate the effects of BG and BS (0.05 g/mL) on the pre-osteoblastic MC3T3-E1 cells, qRT-PCR was performed to measure the expression of genes involved in cell proliferation and differentiation (runt-related transcription factors 2—Runx2 and bone morphogenetic protein 4—BMP4) (Table 1).

MC3T3-E1 were cultured in 24-well (1×10^4 cells/cm^2) plates for 1, 3, and 6 days in contact with the conditioned media previously collected ($n = 5$). Then, after each experimental period, total RNA was isolated using a RNA Isolation Kit (RNeasy Mini Kit, QIAGEN, São Paulo, Brazil). A potential DNA contamination was removed by

Table 1 Primers and the expected PCR product size at indicated annealing temperatures for each gene analyzed

Gene	Forward	Reverse	Annealing temperature (°C)
Runx2	ATGATGAGAACTACTCCGCCG	TGAAACTCTTGCCT CGTCCG	60
BMP4	TTACCTCAAGGGAGTGGAAA TTG	CCATCGTGGCCAAAAGTGA	60
RPS18	ATAGCCTTCGCCATCACTGC	CCCTCTTGGTGAGG TCGATG	60

Runx2, runt-related transcription factor 2; *BMP4*, bone morphogenetic protein 4; and *RPS18*, ribosomal protein S18

RNase-free DNase I (Thermo Fisher Scientific, São Paulo, Brazil). Complementary DNA (cDNA) was generated from the RNA using the High-Capacity cDNA Reverse Transcription Kit (Thermo Fisher Scientific, São Paulo, Brazil). The qRT-PCR analysis was performed on thermal cycler (7500 Fast Real-Time PCR System, Applied Biosystems, Waltham, USA) using SYBR Green detection reagent (Thermo Fisher Scientific, São Paulo, Brazil). Gene relative expression was normalized against the housekeeping gene RPS18 (ribosomal protein S18). Relative expression was calculated using the following formula: $2^{\wedge \text{-}\Delta\Delta Ct}$ (Livak and Schmittgen 2001).

Statistical Analysis

Data were expressed as mean ± standard deviation. Statistical analyses were performed using GraphPad Prism 6 (GraphPad Software, San Diego, CA, USA). Shapiro-Wilk normality test was used to check distribution. Mann-Whitney or Kruskal-Wallis test and Dunn post hoc were used for nonparametric data. t test and one-way analysis of variance (ANOVA) with Tukey multiple comparisons post-tests were used for parametric data. Differences were considered significant at $p \leq 0.05$.

Results

Structural Morphology

SEM micrographs of BS (Fig. 1a) show the characteristic spicules of the species, mostly needle-like structures with smooth surfaces. For BG (Fig. 1b), micrographs showed particles with varied sizes and irregular or angled borders.

FTIR

FTIR spectra for BS and BG showed peaks associated to Si–OH (900–1000 cm^{-1}) and Si–O–Si (near 450 cm^{-1}) bonds (Fig. 2). The characteristic peaks for P=O (1350 cm^{-1}), O–P–O (650 cm^{-1}), and P–O group (at about 500 cm^{-1}) in BG is also shown by the spectra. Additionally, absorption peak for Si–Si was detected at 680 for BS.

XRD

The XRD analysis (Fig. 3) demonstrated the predominant amorphous profile of the BS (Fig. 3a), though silica crystalline peaks were found at Theta Degrees of 20.85, 26.66 and 50.16. No defined crystalline peaks were found for BG (Fig. 3b) due to its completely amorphous character.

Ca Assay

At the first time point, BS showed some mineralization of Ca (~ 85 μg), being statistically different from BG which presented some release of the ion (~ 1088 μg; $p = 0.0176$; Fig. 4). At day 3, the value for BS was statistically different compared to BG which still released some Ca in the solution (~ 1740 μg; $p = 0.0005$). From day 7 until the last time point, a release of Ca was observed for both BS and BG, reaching values of ~ 1660 and ~ 4987 μg at day 21 respectively. Statistically different values were found for BS compared to BG at all these experimental periods, showing that the release of calcium was significantly higher in BG at all time points, as expected ($p = 0.0176, 0.0005, 0.0019, < 0.0001$, and < 0.0001 at days 1, 3, 7, 14, and 21 respectively).

pH Measurements

At day 1, a statistically significant pH decrease was observed for BS (6.80) compared to BG (7.72; $p = 0.0079$; Fig. 5). Similarly, at day 3, a lower pH was found for BS (7.13) compared to BG (7.55; $p = 0.0079$). After this time point, the pH for BS reached a plateau, with values close to 7.2 until the last time point. On the other hand, a relevant pH increase was observed for BG at day 7 (8.56), reaching 8.78 at the last experimental period. Statistical lower pH values were also found for BS compared to BG at days 7, 14, and 21 ($p = 0.0079$).
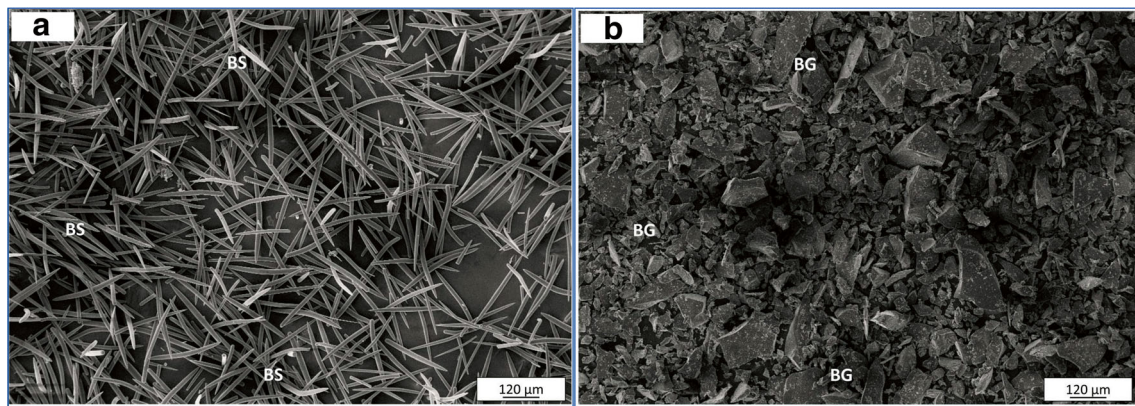
Fig. 1 Representative SEM micrograph of the BS (**a**) and BG (**b**). Spicules of *Dragmacidon reticulatum* with different sizes could be observed for BS. Particles with different sizes were noticed for BG. BS, biosilica; BG, bioglass. Magnification of $\times 200$

Cell Culture Studies

Cytotoxicity studies using alamarBlue indicated that all preconditioned medium with different concentrations of BG and BS (0.1, 0.05, and 0.01 g/mL) did not affect MC3T3-E1 cell viability after 1 and 3 days of culture, since no statistical difference was found when compared to control ($p > 0.05$) (Fig. 6). Interestingly, after 6 days of culture, cell viability was higher in BS 0.05 g/mL compared to control ($p = 0.0048$), BG 0.01 g/mL ($p = 0.0054$), and BG 0.05 g/mL ($p = 0.0001$). Furthermore, BS 0.1 g/mL also presented statistically higher value when compared to BG 0.05 g/mL ($p = 0.0071$) (Fig. 6). No significant difference was observed when comparing all BS concentrations (0.1, 0.05, and 0.01 g/mL; $p > 0.05$). Differently, comparisons among BG groups showed a higher value for BG 0.1 g/mL compared to BG 0.05 g/mL ($p = 0.0117$).

DNA quantification by PicoGreen assay indicated no significant difference among BG, BS groups, and control after 1 and 3 days of culture ($p > 0.05$) (Fig. 7). On the other hand, at the last time point, statistically higher values of DNA amount were found for BS 0.05 g/mL when compared to control ($p = 0.0022$), BG 0.05 g/mL ($p = 0.0007$), BG 0.1 g/mL ($p = 0.0066$), and BS 0.1 g/ml ($p = 0.0008$) (Fig. 7).

Quantitative RT-PCR

Based on the previous results of cytotoxicity and proliferation, the 0.05 g/mL concentration for both BG and BG was chosen to proceed with qRT-PCR analysis. Figure 8 demonstrates Runx2 and BMP4 gene expression for BG 0.05 g/mL and BS 0.05 g/mL after 1, 3, and 6 days of culture.

Regarding Runx2 gene expression, no statistical difference was observed among all groups after 1 and 3 days of culture ($p > 0.05$). However, after 6 days, Runx2 expression was significantly higher on BS 0.05 g/mL in comparison to control ($p = 0.0331$) (Fig. 8a). At the same time point, no other statistical difference was found among groups.

Fig. 2 FTIR spectra for BS and BG. Dashed lines indicate peaks associated to each one of the materials
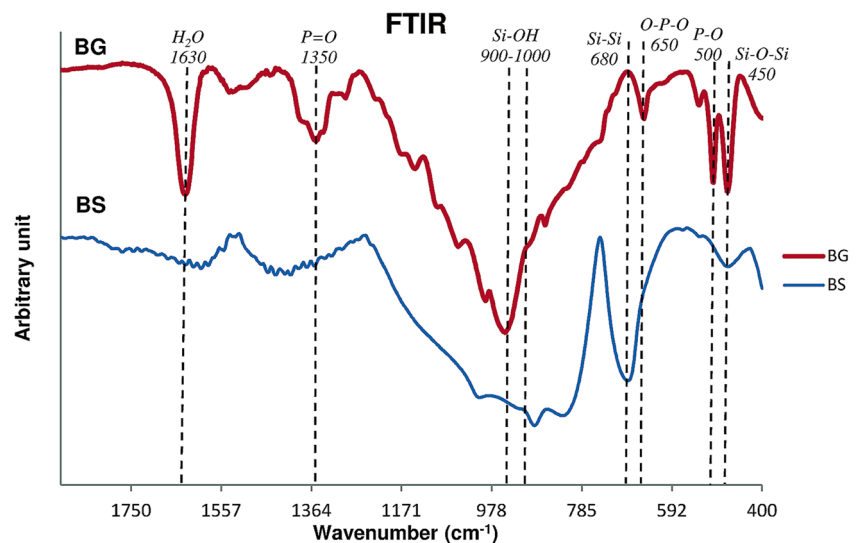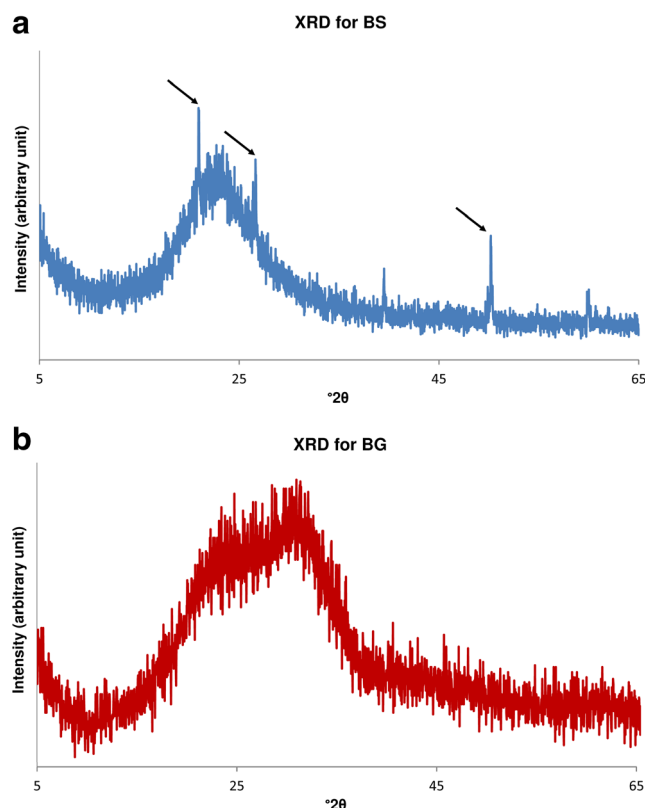
Fig. 3 XRD diffraction pattern for BS (**a**) and BG (**b**). Silica characteristic peaks were observed for BS (arrows; 2-Theta Degrees 20.85, 26.66 and 50.16). No defined crystalline peaks were detected for BG, since it is completely amorphous

Fig. 5 pH measurements for BG and BS. *BG compared to BS ($p = 0.0079$; Mann-Whitney test)

Discussion

The biomimetic potential of marine sponges seems to be a goldmine to material and tissue engineering scientists (Ehrlich and Worch 2007; Granito et al. 2017; Kim 2013; Lin et al. 2011; Muller et al. 2010; Nandi et al. 2015; Rnjak-Kovacina et al. 2015). Some key advantages of BS over BG are: (i) ability to generate silicic acids from much smaller amounts of the bioactive component (Henstock 2009); (ii) similarity with natural extracellular matrix and tunable chemistry (Bonani et al. 2018) and (iii) lower manufacturing and production costs (Granito et al. 2017). In view of that, the present study aimed at obtaining biosilica (BS) and to characterize it morphologic and crystallographically. Moreover, we aimed to investigate bone cell behavior in contact with this mineral, using bioglass as gold standard for comparison purposes (Granito et al. 2017; Hench 2006; Hench 2013). Sponge biosilica was successfully obtained using previous protocol by Weaver et al. (2003) and analyzed by SEM, FTIR, and XRD. Ca assay showed a

For BMP4 gene expression after 1 day of culture, interestingly, BS 0.05 g/mL presented higher expression levels compared to control ($p = 0.0226$) (Fig. 8b). No significant difference was observed when comparing BS 0.05 g/mL with BG 0.05 g/mL. Also, after 3 and 6 days of culture, no statistical difference was found among groups ($p > 0.05$).

Fig. 4 Ca assay for BG and BS. *BS compared to BG ($p = 0.0176$, 0.0005, 0.0019, < 0.0001, and < 0.0001 at days 1, 3, 7, 14, and 21 respectively; t test)
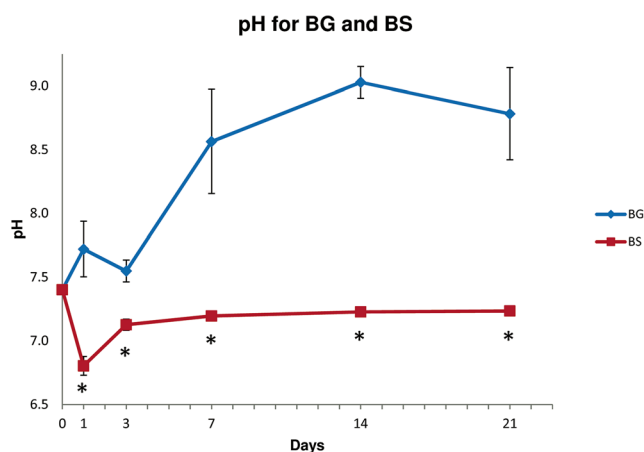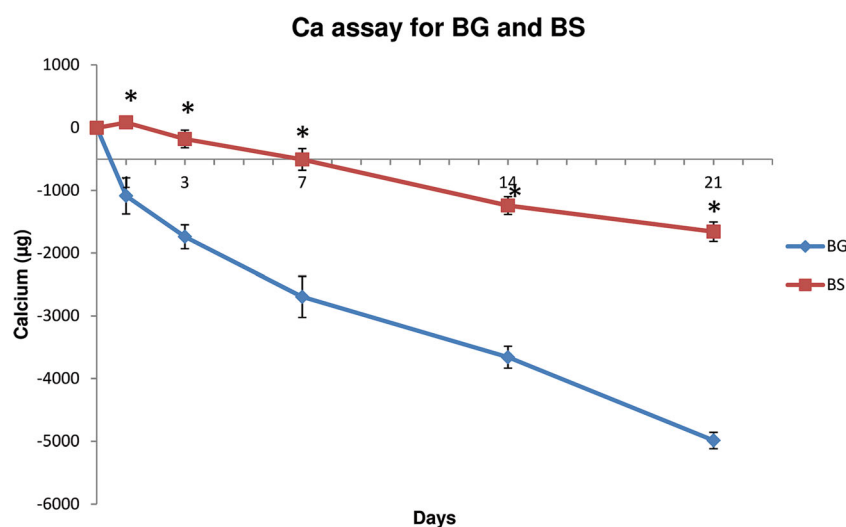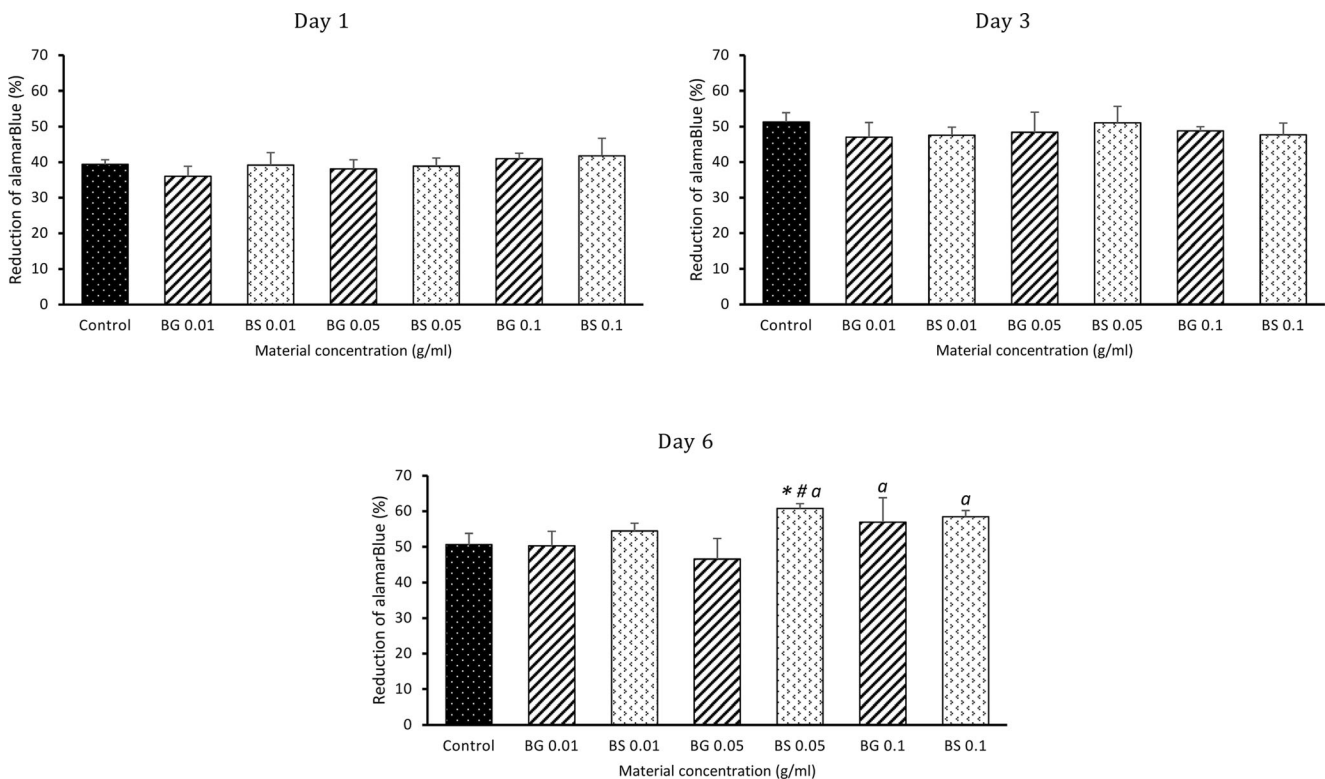
Fig. 6 Cell viability for control, BG (0.01, 0.05, and 0.1 g/ml) and BS (0.01, 0.05, and 0.1 g/ml) after 1, 3, and 6 days of culture. *BS 0.05 g/ml compared to control ($p = 0.0048$; one-way ANOVA analysis); #BS 0.05 g/ml compared to BG 0.01 g/ml ($p = 0.0054$; One-way ANOVA analysis); aBS 0.05 g/ml, BS 0.1 g/ml, and BG 0.1 g/ml compared to BG 0.05 g/ml ($p = 0.0001$, $p = 0.0071$, $p = 0.0117$, respectively; one-way ANOVA analysis)

progressive release of this ion from day 7. A more balanced pH for BS was found compared to BG, with values close to the physiological one. Cytotoxicity assay indicated that BS presented a positive influence on MC3T3-E1 cells viability and qRT-PCR showed that this material stimulated Runx2 and BMP4 expressions. All these results together show to be very promising toward the use of the present biosilica combined with other polymers, ions, and proteins as scaffold for potential treatment of bone defects (Albert et al. 2017; Granito et al. 2017; Guo et al. 2017; Leone et al. 2017; Luo et al. 2017; Müller Werner et al. 2013; Zhu et al. 2018).

Structural morphology investigations by SEM showed mostly intact oxeas and styles, spicule types that compose the inorganic skeleton of the species. These spicules could be originally found composing the inorganic part of the specimen (Croce et al. 2004; Muller et al. 2011; Müller et al. 2009). FTIR assessment for both BS and BG showed Si–OH stretching and Si–O–Si bending peaks which are present in material features silica species (Nariyal et al. 2014). The known P–O bending was also found for BG (Berzina-Cimdina and Borodajenko 2012), as well as P=O (Peitl Filho et al. 1996) and O–P–O (Zarifah et al. 2016) groups. Moreover, peak at 680 cm^{-1} was detected for BS and some authors suggested that this peak is an indicative of a great density of Si–Si bonds (Baierle et al. 1997; Inokuma et al. 1998; Luna-López et al. 2009).

Interestingly, although XRD confirmed the amorphous nature of BS (Schroder et al. 2008; Wang and Müller 2015), some silica crystalline peaks were found (NIOSH 2003) versus the completely non-crystalline BG profile (Rahaman et al. 2011). Most probably, the inherent characteristic of the sponge specie used in this work, made it possible to obtain encapsulated BS within the hierarchical organization and crystalline structure of these spicules. This difference may confer increased mechanical properties for BS compared to BG, which could be attractive, since the latter presents poor mechanical properties (Azenha et al. 2010; Moura et al. 2007). The spicules' composition may enhance fracture toughness, as in the case of the A/W glass-ceramic, composed of an apatite matrix reinforced by needle-like wollastonite crystals (Kokubo 1991; Peitl et al. 2012). Further characterization studies, using other forms of BS obtainment and presentation, are necessary to elucidate this issue.

BS presented an initial mineralization for Ca at day 1 and, in contrast, BG presented release of the ion at this same time point. This may be explained by the phosphate precipitation and initial formation of CaP layer on the surface of the BS particles (Xu et al. 2008). Accordingly, the capacity of biosilica-loaded poly(ϵ-caprolactone) nanofibers active surface to provide the growth and mineralization was already shown by Muller et al. (2014) using osteoclast-like SaOS-2
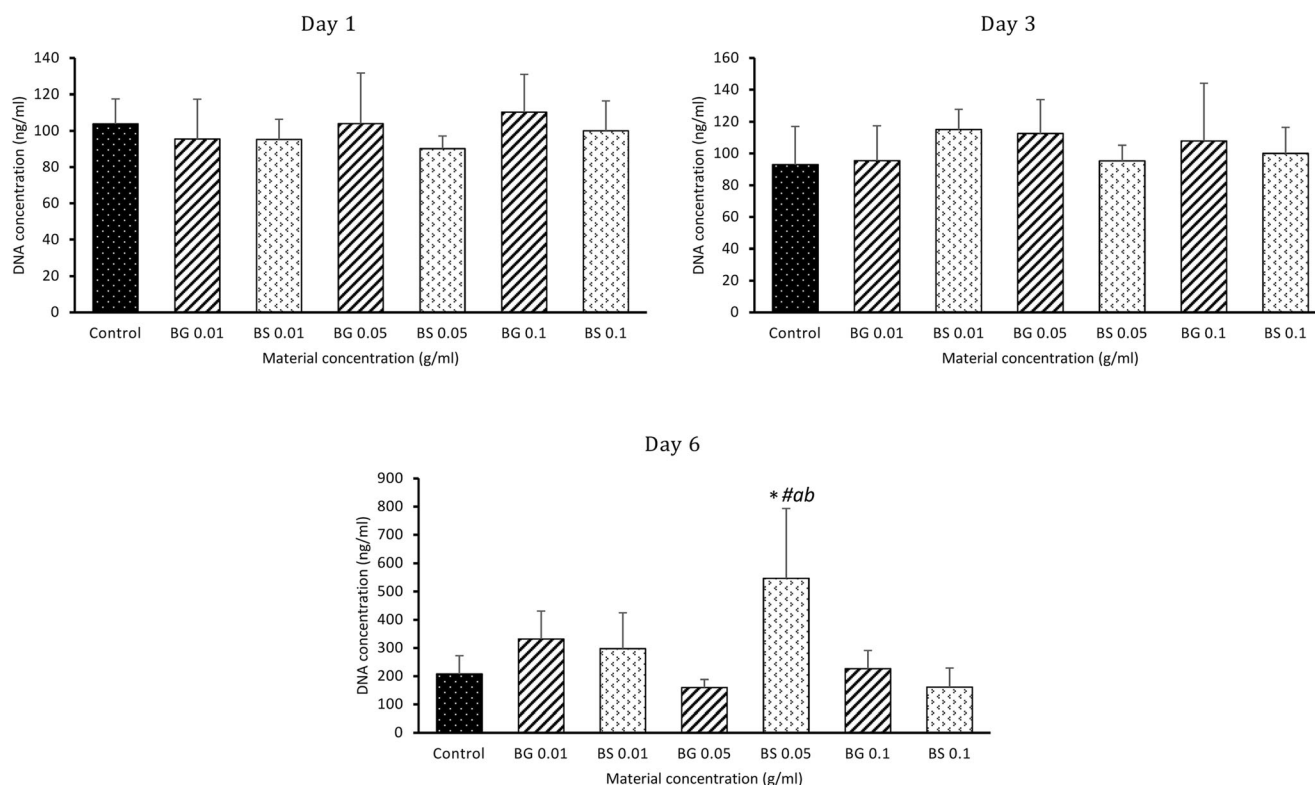
Fig. 7 DNA quantification for control, BG (0.01, 0.05, and 0.1 g/ml) and BS (0.01, 0.05, and 0.1 g/ml) after 1, 3, and 6 days of culture. *BS 0.05 g/ml compared to control ($p = 0.0022$; one-way ANOVA analysis); #BS 0.05 g/ml compared to BG 0.05 g/ml ($p = 0.0007$; one-way ANOVA analysis); aBS 0.05 g/ml compared to BG 0.1 g/ml ($p = 0.0066$; one-way ANOVA analysis); bBS 0.05 g/ml compared to BS 0.1/ml ($p = 0.0008$; one-way ANOVA analysis)

cells (Müller et al. 2014). From day 7, both BS and BG had a continuous release of Ca due to material degradation (Gabbai-Armelin et al. 2014), being more significant for BG. It is suggested that the composition of BG and well-established leaching reactions from this kind of materials, defined by Hench, are responsible for this phenomenon (Hench 2013). Additionally, the controlled release of the ions from BS may have a positive impact on the in vivo behavior of this material (Rahaman et al. 2011).

The pH measurements indicated an initial drop up to 6.80 for BS. Probably, this event may be due to the protocol of biosilica preparation (Weaver et al. 2003), which uses a solution of nitric acid/sulfuric acid to destroy any remaining organic matter, although several washes were performed using Milli-Q water. Nevertheless, after 3 days of incubation, pH for BS reached a plateau, with values close to 7.2. On the other hand, BG had its pH increased to ~7.7 at the first time point, reaching ~8.8 at day 21. Reactions taking place at the BG/solution interface are likely responsible for this change, releasing cations (Si, Ca, Na, and PO_4^{3-}) after the immersion of BG into fluids, thereby leading to an increase in pH (Chen et al. 2008). Taken together, these data show that BS maintain a more balanced pH
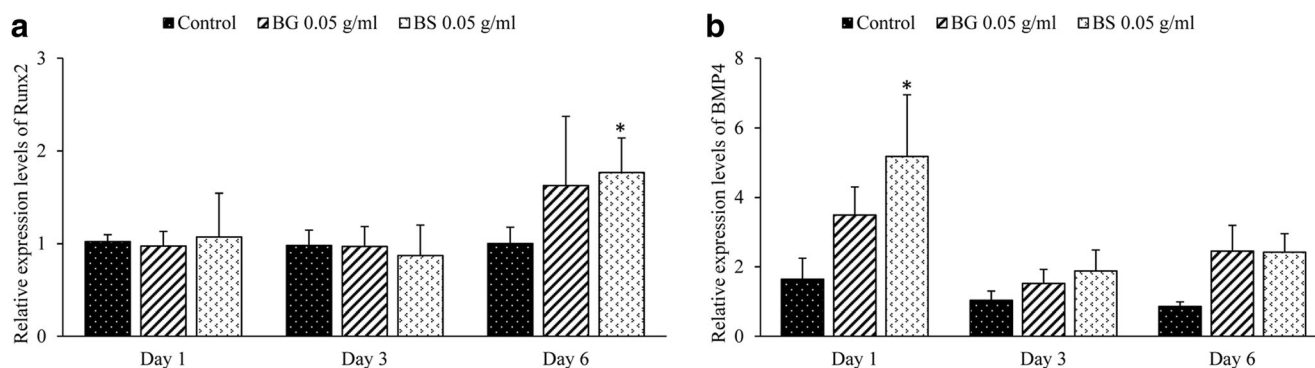

Fig. 8 Relative expression levels of Runx2 (**a**) and BMP4 (**b**) measured by quantitative RT-PCR for BG 0.05 g/ml and BS 0.05 g/ml after 1, 3, and 6 days of culture. *BS 0.05 g/ml compared to control ($p = 0.0331$ and $p = 0.0226$ for Runx2 and BMP4 respectively; Kruskal-Wallis test)

compared to BG when immersed into solution, being close to the physiological pH of 7.4 (Zager et al. 1993).

Cell culture studies by alamarBlue and PicoGreen showed that the sponge biosilica was non-cytotoxic and induced higher cell proliferation, especially at concentration of 0.05 g/mL, compared to control and to the well-known bioglass (Hench 2013). Nandi et al. (2015), investigating cristobalite from the marine sponges *Biemna fortis* via MTT, also demonstrated that this material was non-cytotoxic (Nandi et al. 2015). Following this line, Barros and colleagues, which investigated different marine sponges (*Petrosia ficiformis*, *Agelas oroides*, and *Chondrosia reniformis*) using MTS and PicoGreen assay, showed (i) higher metabolic activity of L929 cells compared to the reference commercial Bioglass® 45S5 (Barros et al. 2016) and (ii) SaOS-2 cells proliferation by DNA quantification, demonstrating that cells are capable to grow and colonize bioceramic structures (Barros et al. 2014). These results indicate the promising utilization of the present ceramic material for biomedical applications, since its degradation products are not cytotoxic, creating a microenvironment suitable for cell viability and proliferation (Yang et al. 2005).

Finally, qRT-PCR of Runx2 and BMP4 was performed with 0.05 g/mL concentration, since it was the most promising one, demonstrating the best results (viability and proliferation) versus control and BG. Runx2 plays a key role on the differentiation of pre-osteoblastic cells to osteoblasts, being a transcriptional regulator critical for bone formation (Hassan et al. 2010; Huang et al. 2007). BMP4, a potent growth factor, which belongs to the transforming growth factor beta superfamily, is also mandatory for inducing ossification, as well as skeletal regeneration (Bragdon et al. 2011; Retzepi et al. 2018). Remarkably, cells in BS 0.05 g/mL showed increased Runx2 and BMP4 expressions compared to control. This indicates that the spicules from marine sponge were capable of inducing cell differentiation toward osteoblastic lineage and could, probably, also induce bone formation in an in vivo scenario. Previous qRT-PCR studies by Wiens and collaborators demonstrated that the growth of human osteoblast–like (SaOS-2) cells on a silicatein/biosilica matrix upregulated BMP2 expression (Wiens et al. 2010). Also, Wang et al. (2014) demonstrated the marine sponge–derived inorganic polymers, biosilica, and polyphosphate, as morphogenetically active matrices/scaffolds for the differentiation of human multipotent stromal cells, revealing that these polymers increased the expression of BMP2 and ALP in osteogenic cells (Wang et al. 2014). Following this line, Werner and co-authors defined silica as a morphogenetically active inorganic polymer, since Na-alginate matrix supplemented with this inorganic silica and embedded with bone- and osteoblast-like SaOS-2 led to the synthesis of hydroxyapatite crystallites by these cells, accompanied by an elevated BMP2 transcript level, and simultaneously also a significant upregulation of the COLI, COLV, OPN, and ON genes (Muller et al. 2013b).

Nevertheless, the same study showed that the steady-state transcript level of Runx2 remained unchanged in the presence of silica, concluding that silica causes its morphogenetic effect with respect to some bone-specific genes in a Runx2-independent way (Muller et al. 2013b). Therefore, additional gene expression analyzes are necessary to elucidate this issue.

Our characterization and cell culture results on biosilica obtained from marine sponges are very inspiring toward further in vivo and in vitro investigations to validate its biological performance for an optimized bone repair.

Conclusions

The present work successfully obtained biosilica from marine sponges with more balanced pH, controlled Ca uptake/release, and increased cell viability/proliferation compared to the amorphous gold standard bioglass. PCR gene expressions showed an upregulation of Runx2 and BMP4 compared to control. Taken together, the results indicate a promising use of sponge biosilica for tissue engineering purposes. Additionally, the present findings are inspiring and lead to in vitro and in vivo studies, using different forms of BS presentation (i.e., composites or scaffolds), to clarify the osteogenic potential and biological performance of this biomaterial.

Compliance with Ethical Standards

Conflict of Interest The authors declare that they have no conflict of interest.

References

Albert K, Huang X-C, Hsu H-Y (2017) Bio-templated silica composites for next-generation biomedical applications. Adv Colloid Interface Sci 249:272–289

American National Standard (ANSI) (1999) Biological evaluation of medical devices — part 5: tests for cytotoxicity, in vitro methods: 8.2 tests on extracts. AAMI Guidance Document ANSI/AAMI/ISO 10995–5

Azenha MR, Peitl O, Barros VMR (2010) Bone response to biosilicates® with different crystal phases. Braz Dent J 21:383–389

Baierle RJ, Caldas MJ, Molinari E (1997) Ossicini S. Optical emission from small Si particles solid state communications 102:545–549

Barros AA, Aroso IM, Silva TH, Mano JF, Duarte ARC, Reis RL (2014) Surface modification of silica-based marine sponge bioceramics induce hydroxyapatite formation. Cryst Growth Des 14:4545–4552

Barros AA, Aroso IM, Silva TH, Mano JF, Duarte AR, Reis RL (2016) In vitro bioactivity studies of ceramic structures isolated from marine sponges. Biomed Mater 11:045004

Berzina-Cimdina L, Borodajenko N (2012) Research of calcium phosphates using fourier transform infrared spectroscopy, infrared spectroscopy theophile theophanides, IntechOpen. https://doi.org/10.5772/36942

Bonani W, Singhatanadgige W, Pornanong A, Motta A (2018) Natural origin materials for osteochondral tissue engineering. In: Oliveira J, Pina S, Reis R, San Roman J (eds) Osteochondral tissue engineering. Advances in Experimental Medicine and Biology, vol 1058. Springer, Cham

Bragdon B, Moseychuk O, Saldanha S, King D, Julian J, Nohe A (2011) Bone morphogenetic proteins: a critical review. Cell Signal 23:609–620

Chen Q, Roether JA, Boccaccini AR (2008) Tissue engineering scaffolds from bioactive glass and composite materials. Topics in Tissue Engineering, vol 4, p 1–27

Croce G, Frache A, Milanesio M, Marchese L, Causà M, Viterbo D, Barbaglia A, Bolis V, Bavestrello G, Cerrano C, Benatti U, Pozzolini M, Giovine M, Amenitsch H (2004) Structural characterization of siliceous spicules from marine sponges. Biophys J 86:526–534

Ehrlich H, Worch H (2007) Sponge as natural composites from biomimetic potential to development of new biomaterials. In: Heidu E (ed) Porifera research: biodiversity, innovation & sustainability, Séries Livros 28. Museu Nacional, Rio de Janeiro, p 217–223

Gabbai-Armelin PR et al (2014) Injectable composites based on biosilicate[registered sign] and alginate: handling and in vitro characterization. RSC Adv 4:45778–45785

Granito RN, Custodio MR, Renno ACM (2017) Natural marine sponges for bone tissue engineering: the state of art and future perspectives. J Biomed Mater Res B Appl Biomater 105:1717–1727

Guo J, Li C, Ling S, Huang W, Chen Y, Kaplan DL (2017) Multiscale design and synthesis of biomimetic gradient protein/biosilica composites for interfacial tissue engineering. Biomaterials 145:44–55

Hak DJ et al (2014) Delayed union and nonunions: epidemiology, clinical issues, and financial aspects. Injury 45(Suppl 2):S3–S7

Hassan MQ et al (2010) A network connecting Runx2, SATB2, and the miR-23a~27a~24-2 cluster regulates the osteoblast differentiation program. Proc Natl Acad Sci U S A 107:19879–19884

Hench LL (2006) The story of bioglass. J Mater Sci Mater Med 17:967–978

Hench LL (2013) Introduction to bioceramics, 2nd ed. Imperial College Press, London, p 620 ISBN: 978–1-908977–15–1

Henkel J et al (2013) Bone regeneration based on tissue engineering conceptions - a 21st century perspective. Bone Res 1:216–248

Henstock JR (2009) Porous silicon–polycaprolactone composites for orthopaedic tissue engineering. University of Nottingham

Huang W, Yang S, Shao J, Li YP (2007) Signaling and transcriptional regulation in osteoblast commitment and differentiation. Front Biosci 12:3068–3092

Inokuma T, Kurata Y, Hasegawa S (1998) Cathodoluminescence properties of silicon nanocrystallites embedded in silicon oxide thin films. J Lumin 80:247–251

Kim SK (ed) (2013) Marine biomaterials: characterization, isolation and applications. CRC Press, Boca Raton, p 840

Kokubo T (1991) Bioactive glass ceramics: properties and applications. Biomaterials 12:155–163

Kokubo T, Takadama H (2006) How useful is SBF in predicting in vivo bone bioactivity? Biomaterials 27:2907–2915

Leone G et al (2017) Ca2+−in vivo doped biosilica from living Thalassiosira weissflogii diatoms: investigation on Saos-2 biocompatibility MRS. Advances 2:1047–1058

Lin Z et al (2011) In vitro evaluation of natural marine sponge collagen as a scaffold for bone tissue engineering. Int J Biol Sci 7:968–977

Livak KJ, Schmittgen TD (2001) Analysis of relative gene expression data using real-time quantitative PCR and the 2(−Delta Delta C(T)) method. Methods 25:402–408

Luna-López JA, Carrillo-López J, Aceves-Mijares M, Morales-Sánchez A, Falcony C (2009) FTIR and photoluminescence of annealed silicon rich oxide films. Superficies y Vacío 22:11–14

Luo H et al (2017) Morphology and cell responses of three-dimensional porous silica nanofibrous scaffold prepared by sacrificial template method. J Non-Cryst Solids 457:145–151

Matassi F, Nistri L, Chicon Paez D, Innocenti M (2011) New biomaterials for bone regeneration. Clin Cases Miner Bone Metab 8:21–24

Matassi F, Carulli C, Civinini R, Innocenti M (2013) Cemented versus cementless fixation in total knee arthroplasty. Joints 1:121–125

Mooren RE, Hendriks EJ, van den Beucken JJ, Merkx MA, Meijer GJ, Jansen JA, Stoelinga PJ (2010) The effect of platelet-rich plasma in vitro on primary cells: rat osteoblast-like cells and human endothelial cells. Tissue Eng A 16:3159–3172

Moura J et al (2007) In vitro osteogenesis on a highly bioactive glass-ceramic (biosilicate). J Biomed Mater Res A 82:545–557

Müller Werner EG, Schröder Heinz C, Feng Q, Schlossmacher U, Link T, Wang X (2013) Development of a morphogenetically active scaffold for three-dimensional growth of bone cells: biosilica–alginate hydrogel for SaOS-2 cell cultivation. J Tissue Eng Regen Med 9:E39–E50

Müller WEG et al (2009) Sponge spicules as blueprints for the biofabrication of inorganic–organic composites and biomaterials. Appl Microbiol Biotechnol 83:397–413

Muller WE, Wang X, Sinha B, Wiens M, Schroder HC, Jochum KP (2010) NanoSIMS: insights into the organization of the proteinaceous scaffold within hexactinellid sponge spicules. Chembiochem 11:1077–1082

Muller WE et al (2011) The unique invention of the siliceous sponges: their enzymatically made bio-silica skeleton. Prog Mol Subcell Biol 52:251–281

Muller WE, Schroder HC, Schlossmacher U, Neufurth M, Geurtsen W, Korzhev M, Wang X (2013a) The enzyme carbonic anhydrase as an integral component of biogenic Ca-carbonate formation in sponge spicules. FEBS Open Bio 3:357–362

Muller WEG et al (2013b) Silica as a morphogenetically active inorganic polymer. Biomater Sci 1:669–678

Müller WEG, Tolba E, Schröder HC, Diehl-Seifert B, Link T, Wang X (2014) Biosilica-loaded poly(ϵ-caprolactone) nanofibers mats provide a morphogenetically active surface scaffold for the growth and mineralization of the osteoclast-related SaOS-2 cells. Biotechnol J 9:1312–1321

Nandi SK, Kundu B, Mahato A, Thakur NL, Joardar SN, Mandal BB (2015) In vitro and in vivo evaluation of the marine sponge skeleton as a bone mimicking biomaterial. Integr Biol 7:250–262

Nariyal RK, Kothari P, Bisht B (2014) FTIR measurements of SiO2 glass prepared by sol-gel technique. Chem Sci Trans 3:1064–1066

NIOSH (2003) Method 7500. Silica crystalline by XRD (filter redeposition). In: Schlecht PC, O'Connor PF (eds) NIOSH manual of analytical methods, 4th edn, issue 4. National institute for occupational safety and health, Cincinnati

Nukavarapu SP, Dorcemus DL (2013) Osteochondral tissue engineering: current strategies and challenges. Biotechnol Adv 31:706–721

Peitl Filho O, LaTorre GP, Hench LL (1996) Effect of crystallization on apatite-layer formation of bioactive glass 45S5. J Biomed Mater Res 30:509–514

Peitl O, Zanotto ED, Serbena FC, Hench LL (2012) Compositional and microstructural design of highly bioactive P2O5-Na2O-CaO-SiO2 glass-ceramics. Acta Biomater 8:321–332

Pressley JC, Kendig TD, Frencher SK, Barlow B, Quitel L, Waqar F (2011) Epidemiology of bone fracture across the age span in blacks and whites. J Trauma 71:S541–S548

Radjasa OK, Vaske YM, Navarro G, Vervoort HC, Tenney K, Linington RG, Crews P (2011) Highlights of marine invertebrate-derived

biosynthetic products: their biomedical potential and possible production by microbial associants. Bioorg Med Chem 19:6658–6674

Rahaman MN, Day DE, Bal BS, Fu Q, Jung SB, Bonewald LF, Tomsia AP (2011) Bioactive glass in tissue engineering. Acta Biomater 7: 2355–2373

Retzepi M, Calciolari E, Wall I, Lewis MP, Donos N (2018) The effect of experimental diabetes and glycaemic control on guided bone regeneration: histology and gene expression analyses. Clin Oral Implants Res 29:139–154

Rnjak-Kovacina J, Wray LS, Burke KA, Torregrosa T, Golinski JM, Huang W, Kaplan DL (2015) Lyophilized silk sponges: a versatile biomaterial platform for soft tissue engineering. ACS Biomater Sci Eng 1:260–270

Schroder HC, Wang X, Tremel W, Ushijima H, Muller WE (2008) Biofabrication of biosilica-glass by living organisms. Nat Prod Rep 25:455–474

Shin H, Quinten Ruhe P, Mikos AG, Jansen JA (2003) In vivo bone and soft tissue response to injectable, biodegradable oligo(poly(ethylene glycol) fumarate) hydrogels. Biomaterials 24:3201–3211

Tsiridis E, Upadhyay N, Giannoudis P (2007) Molecular aspects of fracture healing: which are the important molecules? Injury 38(Suppl 1): S11–S25

Walsh PJ, Clarke SA, Julius M, Messersmith PB (2017) Exploratory testing of diatom silica to map the role of material attributes on cell fate. Sci Rep 7:14138

Wang X, Müller WEG (2015) Involvement of aquaporin channels in water extrusion from biosilica during maturation of sponge siliceous spicules. Biol Bull 229:24–37

Wang X et al (2014) The marine sponge-derived inorganic polymers, biosilica and polyphosphate, as morphogenetically active matrices/ scaffolds for the differentiation of human multipotent stromal cells: potential application in 3D printing and distraction osteogenesis. Mar Drugs 12:1131–1147

Weaver JC, Pietrasanta LI, Hedin N, Chmelka BF, Hansma PK, Morse DE (2003) Nanostructural features of demosponge biosilica. J Struct Biol 144:271–281

Wiens M et al (2010) Osteogenic potential of biosilica on human osteoblast-like (SaOS-2) cells. Calcif Tissue Int 87:513–524

Xu L, Zhang E, Yin D, Zeng S, Yang K (2008) In vitro corrosion behaviour of Mg alloys in a phosphate buffered solution for bone implant application. J Mater Sci Mater Med 19:1017–1025

Yang WD, Gomes RR Jr, Alicknavitch M, Farach-Carson MC, Carson DD (2005) Perlecan domain I promotes fibroblast growth factor 2 delivery in collagen I fibril scaffolds. Tissue Eng 11:76–89

Zager RA, Schimpf BA, Gmur DJ (1993) Physiological pH. Effects on posthypoxic proximal tubular injury. Circ Res 72:837

Zarifah NA, Matori KA, Sidek HAA, Wahab ZA, Salleh MAM, Zainuddin N, Khiri MZA, Farhana NS, Omar NAS (2016) Effect of hydroxyapatite reinforced with 45S5 glass on physical, structural and mechanical properties. Procedia Chem 19:30–37

Zhu W, Gao X, Zou X, Müller WEG, Wang S, Wang Y, Liu Y (2018) Biosilica porous microspheres promote the osteogenic/odontogenic differentiation of human dental pulp cells. J Biomater Tissue Eng 8: 258–266